Binding and Mechanism of Small Molecules Inhibitors of Influenza Virus H3N2 Hemagglutinin: Insights from Molecular Dynamics Simulation

Nadtanet Nunthaboot*, Thitiya Boonma, and Chananya Rajchakom

Multidisplinary Research Unit of Pure and Applied Chemistry and Supramolecular Chemistry Research Unit, Department of Chemistry and Center of Excellence for Innovation in Chemistry (PERCH–CIC), Faculty of Science, Mahasarakham University, Maha Sarakham, 44150, Thailand

Email: nadtanet.n@msu.ac.th (N.N); thitiya.bm@gmail.com (T.B); 65010251004@o365.msu.ac.th (C.R.)

*Corresponding author

Manuscript received April 17, 2024; revised June 1, 2024; accepted July 7, 2024; published October 24, 2024

***Abstract*—Drugs targeting Neuraminidase (NA) and the M2 membrane protein are available in the market, however, their efficacies are significantly impeded by resistances arising from amino acid mutations, posing a major challenge and limiting drug efficiency. Consequently, there is a critical need to explore new drugs that target alternative protein targets. Hemagglutinin (HA), playing a pivotal role in the influenza viral replication cycle, has emerged as an attractive and promising target for the development of novel antiviral drugs. Tert-Butylhydroquinone (TBHQ) was reported to prevent the HA conformational change, thereby inhibiting the HA-mediated entry. Here, molecular dynamics simulations of HA of H3N2 and its inhibitors (TBHQ and derivatives) were performed to investigate their dynamical and structural behaviours. The results show that TBHQ can form more and stronger hydrogen bonds with residues $E57_1$ and $E97_2$, when compared to its analogues. These two residues possibly play a potential stabilizing effect on the HA structure. The results agree well with the predicted and experimental values of binding free energy. The detailed information can provide valuable insights into the structural dynamics of the HA-inhibitor complexes and offer potential avenues for the development of novel antiviral agents targeting influenza virus replication.**

***Keywords*—Hemagglutinin, H3N2 Influenza virus, TBHQ, MD simulation, binding free energy, fusion inhibitor**

I. Introduction

The appearance of the influenza virus has sparked significant global apprehension regarding human health. Historical pandemic outbreaks, such as the 1918 H1N1, 1957 H2N2, and 1968 H3N2 influenza viruses, resulted in millions of deaths. The more recent 2009 H1N1 pandemic, marked by easily detected human-to-human transmission, claimed thousands of lives. Consequently, the imperative to discover and develop anti-influenza agents effective against various influenza virus strains is undeniable.

Among three distinct types (A, B, and C) of influenza viruses, influenza A is the type most associated with pandemics and severe diseases. The influenza A viral particle is characterized by three surface proteins: Hemagglutinin (HA), Neuraminidase (NA), and the transmembrane protein M2. The integral membrane protein M2 serves multiple functions, including proton selection and ion channel activities. HA and NA play distinct roles in the influenza virus life cycle: HA facilitates viral entry into target cells, while NA is responsible for the release of newly synthesized viral particles. Presently, clinically available anti-influenza drugs target NA (oseltamivir, zanamivir, peramivir, and laninamivir) and the M2 membrane channel (amantadine and rimantadine) [1]. However, the effectiveness of these drugs is limited due to the emergence of drug resistance resulting from amino acid mutations [2, 3]. Consequently, there is an ongoing effort to discover new potent inhibitors against novel targets.

Given its pivotal role in the influenza viral replication cycle, the primary surface glycoprotein, HA, has emerged as an appealing target for the design and development of anti-influenza drugs and vaccines [4]. The HA monomer undergoes synthesis as a precursor polypeptide (HA0) and is subsequently proteolytically cleaved into two disulfide-linked polypeptide chains, HA1 and HA2, (Fig. 1).

Following the binding of HA1 to the receptor on the host membrane, the virus is internalized into cells through endocytosis. Within the acidic pH conditions of the endosome, a significant and irreversible conformational rearrangement occurs in HA. During this process, the membrane distal HA1 domain undergoes de-trimerization and separates from the HA2 fusion domain, except for a disulfide tether. Subsequently, the fusion peptide, located at residues 1–20 in the N terminus of the HA2 subunit, is released from the interior of HA2 at neutral pH, inserting into the endosomal membrane of the host organ. This event promotes viral infectivity and the spread of the influenza virus. As the exposure of the fusion peptide is crucial for the fusion process, the identification of compounds that block this event represents one of the potential strategies for antiviral intervention.

Of the HA fusion inhibitors, Tert-Butyl Hydroquinone (TBHQ) currently stands out as one of the most potent compounds, exhibiting inhibitory effects on the conformational rearrangement of the H3N2 virus with IC_{50} values ranging between 5 to 10 μM [5]. Recent co-crystal structures of TBHQ bound to H3 and H14 HAs have been reported, revealing that the inhibitor binds within a hydrophobic area at the interface between HA protomers (Fig. 1) [6]. TBHQ interferes with virus infectivity by impeding the low pH-induced conformational change of HA into its fusogenic state. In doing so, it prevents the fusion between the virus and the host cell membrane.

To investigate the structural and dynamical behaviors of the protein-ligand complex, Molecular Dynamics (MD) simulations were conducted on the system involving HA bound with TBHQ. Additionally, in an effort to elucidate the differences in inhibitory potency among TBHQ and its

related compounds, molecular dynamics simulations were carried out for its TBHQ derivatives (TB2 and TB3). The results were analyzed, focusing on intermolecular hydrogen bonds and the binding free energy of the complex The detailed information can contribute essential insights into drug-target interactions, offering valuable information for the future design of novel and potent fusion inhibitors targeting group 2 HAs.

II. Literature Review

Russell and colleagues [6] successfully captured the complex structure of H3 H14 group proteins and TBHQ, which inhibits membrane fusion. They discovered that TBHQ binds to the hydrophobic pocket formed by the interface of each HA protomer. TBHQ functions to stabilize the HA protein structure at neutral pH, employing intersubunit and intrasubunit reactions to prevent conformational changes that lead to membrane fusion. Moreover, they compared why TBHQ was effective against group 2 HAs (H3, H4, H14, H7, H15, and H10) but not against group 1 HAs (H9, H8, H12, H6, H2, H5, H1, H11, H16, and H13). The rationale is attributed to the unfavorable positioning of Lys58 in group 1 HAs due to increased helical content, leading to the formation of an intersalt bridge between Lys58 and Glu97. This interaction is absent in group 2 HAs, creating a suitable binding site for TBHQ. Besides TBHQ, arbidol was found to act by binding to the HA protein before the fusion step, forming a complex with the protein and impeding the interaction with the host cell membrane. This interaction stabilized the complex and prevented further fusion events [7, 8].

Recently, MD simulations of various inhibitors and different HA subtypes at different pH (pH = 5–7) were performed to investigate the conformational change of HA2 protein [9]. Among all inhibitors, stachyflin showed higher binding for all HA subtypes of influenza A virus. The MD simulation revealed that stachyflin's performance is enhanced when it directly interacts with residues at the intramonomer binding site rather than the intermonomer binding site. The susceptibility of the HA2 protein of different subtypes to stachyflin follows the order of H1 > H7 > H5 > H2 > H3. Stachyflin exhibits a higher binding affinity for H1 (at pH 7, pH 6, pH 5) and H7 subtypes compared to others. Key residues, namely K47, K58, and E103, play a critical role in facilitating binding and highly stabilizing the HA2 protein at low pH.

In the previous study, Boonma *et. al.* [10] performed MD simulations of H3N2 HA complexed with ardidol and its dertivative, der-arbidol, and found that arbidol derivative formed multiple strong hydrogen bonds with surrounding HA amino acids, including E1032(1), K3071(1), and K3102(1), while arbidol interacted in a similar way with only K582(1). The addition of a hydroxyl group at the meta-position of the thiophenol ring was observed to displace a nearby water molecule. This displacement facilitated direct hydrogen bond formation between der-arbidol and E1032(1) of the HA residue. Moreover, The stability of salt bridge networks, specifically among residues E572(1) · R542(1) · E972(2), was significantly higher in the case of HA-Der-arbidol compared to that observed in HA-Arbidol.

III. Materials and Methods

Construction and optimization of the inhibitors were carried out using the HF/6-31G* level of theory through the Gaussian 03 program [11]. Subsequently, atomic partial charges were computed using the Restrained Electrostatic Potential (RESP) method. The topology for all three inhibitors was then generated using the antechamber module of the Amber14 package [12].

The protein structure of homo trimeric H3N2 complexed with TBHQ was retrieved from the PDB databank (PDB code: 3EYM) (6). The structures of TB2 and TB3 share a similar scaffold to that of TBHQ, therefore, the structures of H3N2 HA complexed with derivatives (TB2 and TB3) were modified from that of TBHQ. The trimeric HAs bound to inhibitors were then subjected to further MD simulation to investigate the structural dynamics and the role of amino acids in the binding energy. The protein and ligand were described by ff14SB [13] and gaff parameters [14], respectively.

The MD simulations were carried out using the Amber14 software. The LEaP module was employed to add all hydrogen atoms to the protein. Each protein-ligand complex was immersed into the cubic box of TIP3P water molecules, employing periodic boundary conditions extending to 10 Å from the complex. Sodium counter ions were added to neutralize the systems. These solvated systems served as the starting structure for the subsequent MD simulation.

Prior to MD simulations, an energy minimization process was conducted for each system, involving 2000 steps of the Steepest Descent (SD) algorithm followed by 3000 steps of the Conjugate Gradient (CG) algorithm. Subsequently, the system was heated from 10 K to 310 K over 50 ps. MD simulations were then carried out under a constant temperature and pressure ensemble (NPT), with a constant pressure of 1 atm and a constant temperature of 310 K. The Berendsen thermostat was employed to maintain the temperature. Long-range electrostatic interactions were described using the Particle Mesh Ewald approach [15], with a spherical cutoff of 10.0 Å for non-bonded interactions. Bonds involving hydrogen were constrained using the SHAKE algorithm [16]. MD simulations were performed for a total of 100 ns, and trajectories collected during the last 50 ns were analyzed to investigate time-dependent characteristics and energetic stabilization.

IV. Result and Discussion

The experimentally resolved X-ray structure of H3N2 HA in complex with TBHQ indicated that the ligand located at the interface between two protomers of the HA trimer (3 TBHQ sites per trimer). Contribution of protein-ligand is predominantly from hydrophobic interaction by the conserved residues L291(A), L982(A) of protomer A, and L992(B) of protomer B (subscripts 1 and 2 denotes a residue from HA1 and HA2, respectively). There are three ionizable amino acids; R541, E571 and E972 positioned in the inhibitor binding area. Although only E571 was apparently observed to establish hydrogen bond with ligand, this kind of interaction was considerably different for each inhibitor binding site. At each HA dimer interface, the O2H group of TBHQ was buried inside the active cavity while the O1H

oriented outside the pocket and partially exposed to solvent. TBHQ located at site 2 (between protomers B and C) and 3 (between protomers A and C) could possibly form hydrogen bond interaction with the side chain of E571 while no specific interaction between ligand and E572 at site 1 (between protomers A and B) was detected. Due to the high flexibility of E571, this charge residue of the three HA protomers exhibited different orientation. At sites 2 and 3, the orientation of E571 side chain was originally appropriate to make a hydrogen bond (ca. 4.3 Å) with ligand while the distance at site 1 was relatively large (ca. 6.3 Å) to form such kind of interaction. This therefore could affect the different patterns of interaction between TBHQ and HA at the binding interfaces of the three protomers.

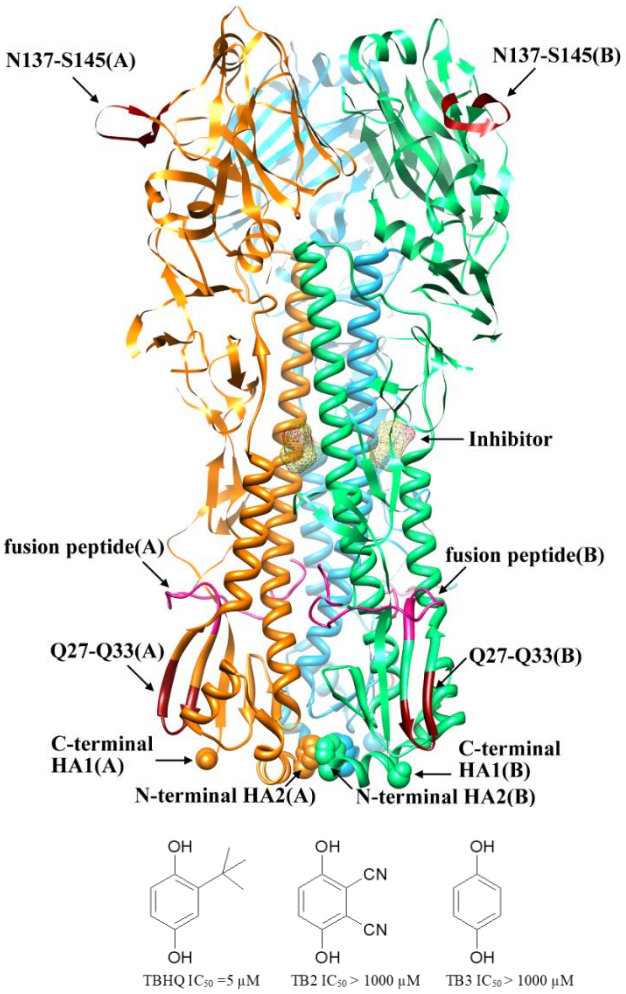

Fig. 1. (top) The three-dimension of trimeric-HA. The HA1 is shown in flat ribbon and the HA2 is rounded ribbon. The red regions are the high flexibility amino acid residue, while the pink colored is fusion peptide. The orange ribbon is HA subunit-A, green is subunit-B and blue colored is subunit-C. (bottom) Chemical structures and biological activities of TBHQ, TB2 and TB3.

A. Protein-ligand Interactions

The hydrogen bond formation between ligand and its nearby HA residues were analyzed during the simulation period and the results were given in Fig. 2. Different hydrogen bond behaviors were observed among H3N2 HA in complex with each inhibitor. Clearly, among the three compounds, TBHQ exhibited larger numbers and stronger hydrogen bond interactions with HA virus than its analogue compounds. After simulation, the O1H of TBHQ created direct hydrogen bonds with the side chain of E572 for the three binding sites while the tert-butyl part was stabilized by hydrophobic interactions with non-polar residues such as L982(A), V1002(A), Y942(B), L992(B), and A1012(B).

Compared to THBQ, interaction between HA and the other two analogue compounds, TB2 and TB3, were significantly weakened. There was only one hydrogen bond formation between E571 and TB2 at site 3. The present of cyanide moiety did not involve in the interaction between protein-ligand complexes. Since no non-polar substituent in TB2, hydrophobic interaction was totally disappeared. In the case of TB3, two weak hydrogen bonds between ligand and R541 at site 2 or E972 at site 2 were found. Due to the absence of hydrophobic substituent group, ligand completely loosed hydrophobic interactions with the surrounding residues. Overall, both the hydrophobic and hydrogen bonding are key elements for the interaction between H3N2 HA and its inhibitor. Therefore, the differences in the hydrophobic and hydrogen bonding patterns among the three compounds could cause their different activities. Based on the above information, we hypothesized that compounds that could form hydrogen bonds with both E571 of one HA protomer and E972 of another protomer may effectively stabilize the neutral pH structure of HA, thereby preventing its conformational rearrangement necessitated for membrane fusion.

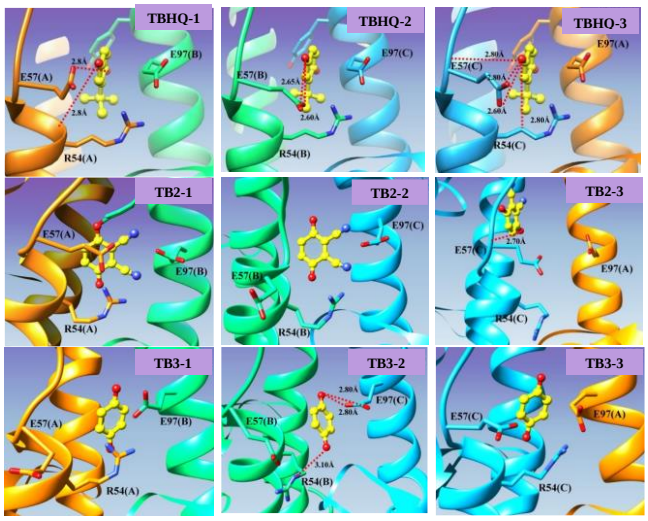

Fig. 2. Binding modes of (top) TBHQ, (middle) TB2 and (bottom) TB3 at three different binding interface of HA trimer.

B. Binding Free Energy Calculation

The binding free energy changes upon binding of inhibitors are given in Table 1. A hundred snapshots of protein bound inhibitors of the last 50 ns were analyzed. The TBHQ inhibitor was experimentally reported to be the most potent compound among the three inhibitors. Both *van der Waals* and electrostatic energies comparatively contributed to the binding of TBHQ. However, in the case of TB2 system, the main contribution to the binding was mainly from *van der Waals* interaction while the electrostatic energy played a major role to stabilize the TB3 complex.

The calculated binding free energies of the HA-TBHQ, HA-TB2 and HA-TB3 were −8.96, −3.21 and −4.57 kcal/mol, respectively, suggesting stronger binding affinity of TBHQ to H3N2 HA. The non-polar solvation free energy arising from

the burial of the solvent accessible surface area upon ligand binding slightly contributed to the binding energy. However, the polar solvation term produced unfavourable component to the overall binding free energy. The order of magnitude for the averaged binding free energy was TBHQ > TB2 > TB3, consistent with the experimental measurements.

Table 1. The MM/PBSA binding free energies and their energy contributions (in kcal/ mol) as well as the estimated experimental binding free energies for TBHQ, TB2 and TB3.

System	TBHQ			TB2			TB3		
	Site-1	Site-2	Site-3	Site-1	Site-2	Site-3	Site-1	Site-2	Site-3
$\langle \Delta E_{elec} \rangle_{AV}$	−19.07 (7.82)	−20.07 (3.35)	−22.79 (6.95)	−17.67 (4.00)	−25.69 (3.23)	−50.73 (4.92)	−5.86 (2.63)	−9.95 (6.26)	−7.65 (5.15)
$\langle\langle \Delta E_{elec} \rangle\rangle_{AV}$		−20.64			−31.36			−7.82	
$\langle \Delta E_{vdw} \rangle_{AV}$	−22.5 (3.70)	−18.75 (2.18)	−18.94 (2.46)	−21.7 (1.63)	−25.4 (1.72)	− 17.75 (2.00)	−17.57 (1.37)	−16.37 (1.9)	−15.57 (1.50)
$\langle\langle \Delta E_{vdw} \rangle\rangle_{AV}$		−20.06			−21.62			−16.50	
$\langle \Delta E_{MM} \rangle_{AV}$	−41.56 (6.25)	−38.82 (2.85)	−41.65 (6.13)	−39.37 (4.41)	−51.08 (3.74)	−68.47 (4.45)	−23.42 (2.87)	−26.32 (6.03)	−23.22 (5.07)
$\langle\langle \Delta E_{MM} \rangle\rangle_{AV}$		−40.68			−52.97			−24.32	
$\langle \Delta G^{0}_{nonpol} \rangle_{AV}$	−3.87 (0.74)	−3.80 (0.1)	−3.53 (0.17)	−3.25 (0.38)	−3.16 (0.11)	−2.95 (0.08)	−2.66 (0.08)	−2.63 (0.19)	−2.49 (0.4)
$\langle\langle \Delta G^{0}_{nonpol} \rangle\rangle_{AV}$		−3.72			−3.12			−2.59	
$\langle \Delta G^{0}_{pol} \rangle_{AV}$	36.03 (7.30)	36.29 (4.46)	34.03 (6.73)	47.96 (7.84)	51.02 (5.72)	59.67 (4.23)	21.22 (5.09)	23.74 (3.95)	22.06 (4.72)
$\langle\langle \Delta G^{0}_{pol} \rangle\rangle_{AV}$		34.45			58.88			22.34	
$\langle \Delta G^{0}_{sol} \rangle_{AV}$	32.17 (7.11)	32.48 (4.43)	30.50 (6.68)	44.71 (7.85)	47.87 (5.71)	56.72 (4.22)	18.56 (5.08)	21.11 (3.96)	19.57 (4.73)
$\langle\langle \Delta G^{0}_{sol} \rangle\rangle_{AV}$		31.72			50.10			19.75	
$\langle \Delta G^{0}_{bind} \rangle_{PBSA}$	−9.40 (5.36)	−6.34 (3.97)	−11.15 (3.97)	−5.33 (5.95)	−3.22 (4.36)	−11.75 (2.48)	−4.86 (4.34)	−5.21 (5.21)	−3.65 (4.07)
$\langle\langle \Delta G^{0}_{bind} \rangle\rangle_{PBSA}$		−8.96			−6.76			−4.57	
$\Delta G^{*}_{experiment}$		−7.2			−4.1			−4.1	

* Estimated from experimental IC_{50} (ΔG= RT ln IC_{50})

V. Conclusion

HA, playing a crucial role in the influenza viral replication cycle, has emerged as an attractive target. A small molecule TBHQ has been reported to prevent the HA conformational change, thereby inhibiting HA-mediated entry and presenting a potential avenue for novel antiviral interventions. Here, MD simulations of H3N2 HA complexed with TBHQ, and its derivatives (TB2 and TB3) were conducted. TBHQ demonstrated a higher number and stronger hydrogen bond interactions with the HA virus compared to its analogue compounds. Both hydrophobic and hydrogen bonding interactions are the key elements to stabilize HA and its fusion inhibitors. Our hypothesis posits that compounds capable of forming hydrogen bonds with both $E57_1$ of one HA protomer and $E97_2$ of another protomer may effectively stabilize the neutral pH structure of HA. This stabilization, in turn, would prevent the conformational rearrangement necessary for membrane fusion to occur.

Conflict of Interest

The authors declare no conflict of interest.

Author Contributions

Nadtanet Nunthaboot conducted the research and wrote the paper. Thitiya Boonma analyzed the data. Chananya Rajchakom produced figures and graphics. All authors had approved the final version.

Funding

This research project was financially supported by the Thailand Science Research and Innovation (TSRI).

Acknowledgment

N.N. would like to thank the Center of Excellence for Innovation in Chemistry (PERCH-CIC) for financial support. Supramolecular Chemistry Research Unit (Mahasarakham University) and the Structural and Computational Biology Research Unit (Chulalongkorn University) are acknowledged for computational facilities.

References

[1] M. G. Ison, "Antivirals and resistance: Influenza virus," *Curr. Opin. Virol.*, vol. 1, pp. 563–573, 2011. doi: 10.1016/j.coviro.2011.09.002

[2] R. A. Bright, D. K. Shay, B. Shu, N. J. Cox, and A. I. Klimov, "Adamantane resistance among influenza a viruses isolated early during the 2005–2006 influenza season in the United States," *J. Am. Med. Assoc.*, vol. 295, pp. 891–894, 2006. doi: 10.1001/jama.295.8.joc60020

[3] V. M. Deyde, X. Xu, and R. A. Bright *et al.*, "Surveillance of resistance to adamantanes among influenza A(H3N2) and A(H1N1) viruses isolated worldwide," *J. Infect. Dis.*, vol. 196, pp. 249–257, 2007. doi: 10.1086/518936

[4] T. Horimoto and Y. Kawaoka, "Influenza: lessons from past pandemics, warnings from current incidents," *Nat. Rev. Microbiol*., vol. 3, pp. 591–600, 2007. doi: 10.1038/nrmicro1208

[5] A. Antanasijevic, N. J. Hafeman, and S. Tundup *et al.*, "Stabilization and improvement of a promising influenza antiviral: Making a PAIN PAINless," *ACS Infect. Dis.*, vol. 2, pp. 608–615, 2016. doi: 10.1021/acsinfecdis.6b00046

[6] R. J. Russell, P. S. Kerry, and D. J. Stevens *et al.*, "Structure of influenza hemagglutinin in complex with an inhibitor of membrane fusion," *PNAS*, vol. 105, pp. 17736–17741, 2008. doi: 10.1073/pnas.0807142105

[7] I. A. Leneva, R. J. Russell, Y. S. Boriskin, and A. J. Hay, "Characteristics of arbidol-resistant mutants of influenza virus: Implications for the mechanism of anti-influenza action of arbidol," *Antiviral Res.*, vol. 81, pp. 132–140, 2008. doi: 10.1016/j.antiviral.2008.10.009

[8] R. U. Kadam and I. A. Wilson, "Structural basis of influenza virus fusion inhibition by the antiviral drug Arbidol," *Proc. Nat. Acad. Sci. USA.*, vol. 114, pp. 206–214, 2017. doi: 10.1073/pnas.1617020114

[9] S. Kannan, R. Shankar, and P. Kolandaivel, "Insights into structural and inhibitory mechanisms of low pH-induced conformational change of influenza HA2 protein: A computational approach," *J. Mol. Model.*, vol. 25, 2019. doi: 10.1007/s00894-019-3982-y

[10] T. Boonma, N. Soikudrua, B. Nutho, T. Rungrotmongkol, and N. Nunthaboot, "Insights into binding molecular mechanism of hemagglutinin H3N2 of influenza virus complexed with arbidol and its derivative: A molecular dynamics simulation perspective," *Comput. Biol. Chem.*, vol. 101, 107764, 2022.

[11] M. J. Frisch, G. W. Trucks, and H.B. Schlegel *et al.*, *Gaussian 09, Revision C.01*, Gaussian Inc., Wallingford CT, 2009.

[12] D. A. Case, V. Babin, and J. T. Berryman *et al.*, *AMBER 14*, University of California, San Francisco, 2014.

[13] J. A. Maier, C. Martinez, K. Kasavajhala, L. Wickstrom, K. E. Hauser, and C. Simmerling, "ff14SB: Improving the accuracy of protein side chain and backbone parameters from ff99SB," *J. Chem. Theory Comput.*, vol. 11, pp. 3696–3713, 2015. doi: 10.1021/acs.jctc.5b00255

[14] J. Wang, R. M. Wolf, J. W. Caldwell, P. A. Kollman, and D. A. Case, "Development and testing of a general Amber force field," *J. Comput. Chem.*, vol. 25, pp. 1157–1174, 2004. doi: 10.1002/jcc.20035

[15] T. Darden, D. York, and L. Pedersen, "Particle mesh Ewald: An N·log(N) method for Ewald sums in large systems," *J. Chem. Phys.*, vol. 98, pp. 10089–10092, 1993. doi: 10.1063/1.464397

[16] J. P. Ryckaert, G. Ciccotti, and H. J. C. Berendsen, "Numerical integration of the cartesian equations of motion of a system with constraints: molecular dynamics of n-alkanes," *J. Comput. Phys.*, vol. 23, pp. 327–341, 1977. doi: 10.1016/0021-9991(77)90098-5